



# Mathematical functions for optimisation of conducting polymer/activated carbon asymmetric supercapacitors

Graeme A. Snook<sup>1</sup>, Gregory J. Wilson\*, Anthony G. Pandolfo

CSIRO Energy Technology, Box 312, Clayton, Vic. 3169, Australia

## ARTICLE INFO

### Article history:

Received 23 April 2008

Received in revised form 5 August 2008

Accepted 5 September 2008

Available online 2 October 2008

### Keywords:

Electrochemical double-layer capacitor

Ultracapacitor

Asymmetric supercapacitor

Hybrid supercapacitor

Electrically conducting polymer

## ABSTRACT

Equations routinely used to describe the properties of conventional symmetric electrochemical double-layer capacitors (EDLCs) are expanded to develop straightforward mathematical functions that can effectively describe the performance characteristics of asymmetric supercapacitors based on electrically conducting polymer and activated carbon (ECP-AC) electrodes. Formulae are developed to describe cell parameters (based on total active material mass) such as maximum specific capacitance ( $\text{Fg}^{-1}$ ), maximum specific energy ( $\text{Whkg}^{-1}$ ), and optimum electrode mass ratios that can be used for maximising the specific energy of asymmetric cells. The electrode mass ratios are found to have a significant impact on the swing voltages across the positive and negative electrodes. Illustrative EDLC and ECP-AC devices are explored and employed to verify the derived equations that serve to predict essential parameters of both symmetric and asymmetric systems, irrespective of electrolyte ion concentration, solvent or species and independent of voltage. The utility of the equations is demonstrated by predicting cell parameters for a number of theoretical asymmetric ECP-AC systems and used to correlate experimentally obtained parameters.

© 2008 Elsevier B.V. All rights reserved.

## 1. Introduction

Ultracapacitor, or supercapacitor, is a generic term given to a versatile class of energy storage devices that rely on the physical adsorption of ions at an electrode|electrolyte interface to form an electric double-layer; hence the more specific term of electrochemical double-layer capacitor (EDLC) [1]. The most highly developed commercial form of a supercapacitor is the symmetric carbon EDLC, which consists of two identical porous electrodes separated by an ion-permeable separator and electrolyte. These devices are characterised by rapid charge and discharge capabilities, high specific power, good stability, and a lifetime of greater than 500 000 deep charge–discharge cycles.

Traditionally, porous activated carbon (AC) is utilised as the active electrode material in these devices due to its high porosity (electrolyte accessibility), good conductivity, low cost, and high surface area. A wide range of activated carbons, with BET surface areas of up to  $\sim 3000 \text{ m}^2 \text{ g}^{-1}$ , has been evaluated in supercapacitors [2–4], and whilst higher capacitances are theoretically achievable for this material [1,5], in practice, the upper limit for the measured capacitance of activated carbon (on a single electrode basis) is generally

around  $\sim 130 \text{ Fg}^{-1}$  in non-aqueous electrolytes, and  $\sim 200 \text{ Fg}^{-1}$  in aqueous electrolytes [6,7].

The energy stored by a supercapacitor is given by

$$E = \frac{1}{2} CV^2 \quad (1)$$

where  $C$  is the capacitance and  $V$  is the voltage. Therefore, to improve the amount of energy stored in a supercapacitor that is already operating at  $V_{\text{max}}$ , an increase in the gravimetric capacitance of the electrodes and/or a decrease in volume is necessary. The total (cell) capacitance,  $C_T$ , of a symmetric EDLC, with two porous electrodes in series, is given by

$$\frac{1}{C_T} = \frac{1}{C_1} + \frac{1}{C_2} \quad (2)$$

where  $C_1$  and  $C_2$  refer to the double-layer capacitance at each individual electrode. For identical capacitance electrodes, therefore, the total cell capacitance equals half the individual electrode capacitance, *i.e.*,  $C_T = \frac{1}{2} C_1$ . One method to overcome the limitation identified by the above relationship, and also to increase the energy of the cell, is to substitute one of the porous electrodes with a very high capacitance material to form an ‘asymmetric cell’. Thus, for example, if  $C_2 \gg C_1$ , then  $1/C_T \approx 1/C_1$  and so  $C_T \approx C_1$ . That is, the asymmetric cell now has almost twice the capacitance of a comparable symmetric cell in which both the electrodes utilise the same porous carbon.

\* Corresponding author. Tel.: +61 395458632; fax: +61 395628919.

E-mail address: [Greg.Wilson@csiro.au](mailto:Greg.Wilson@csiro.au) (G.J. Wilson).

<sup>1</sup> Current address: CSIRO Minerals, Box 312, Clayton South, Vic. 3169, Australia.

Asymmetric supercapacitors (also sometimes referred to as hybrid supercapacitors), which incorporate dissimilar electrode materials within a single cell, have gained considerable attention over the past few years. The most common form consist of a porous EDLC electrode in series with a 'battery-like' electrode [8–12]. In such a device, the latter electrode contains an active material that undergoes a reversible redox process as the primary mode of energy storage and shows only a relatively small voltage variation during discharge (which effectively has a very high capacitance), so that the cell capacitance approaches that of the porous (capacitive) electrode. The challenge in this device is to optimise both the type and the ratio of the electrode materials so that the asymmetric device achieves an increased specific energy whilst still maintaining the favourable attributes of symmetric devices such as rapid charge capability and very long cycle-life.

Electrically conducting polymers (ECPs) are a class of redox materials often utilised as alternative, high capacitance, electrode materials in supercapacitors due to their inherently fast pseudo-capacitive properties [13–15] and versatile methods of production [16,17]. The rapid, reversible Faradaic processes that occur within ECPs arise from oxidation and reduction (redox processes) of the polymeric material. Hence, the resultant doping and de-doping of the polymeric backbone by ions in the electrolyte, which mimic electrostatic capacitance, can provide enhanced capacitive behaviour when cycled within the stable electrochemical window of the material [18–22]. Polypyrrole (PPy) and polyaniline (PAni) are examples of two ECPs that have been extensively evaluated as active materials in capacitors with reported specific capacitances of  $\sim 250$  and  $500 \text{ F g}^{-1}$ , respectively [23]. A typical asymmetric ECP-AC capacitor involves the substitution of one porous activated carbon electrode with an electrode containing ECP as the main active material.

In order to understand the operational characteristics of asymmetric supercapacitors, several groups have made significant contributions concerning the configuration and optimisation of these energy storage devices. Pell and Conway [24] described and compared hybrid systems with that of a symmetric EDLC and related the device functions to a series of defining equations, by the examination of the conditions required for maximum energy and power, at a maximum voltage. Over the past decade, a series of papers have been published by Zheng and co-workers [25–29], where a theoretical model has been developed for the description of asymmetric capacitors that have a battery-type electrode in series with an AC electrode. These reports, and the model developed, have emphasised a maximum theoretical specific energy, and incorporate important cell parameters such as the respective specific electrode capacities, ionic strength, and the swing potential of the AC electrode. In a similar study on aqueous asymmetric cells, Kazaryan et al. [30] have undertaken a detailed mathematical study to develop a model for heterogeneous supercapacitors that allows calculation of many cell parameters including energy, capacity and power density.

A limitation of the asymmetric model proposed by Zheng [28] and others is that only the swing of the negative (or capacitive) electrode potential is factored into the model and, consequently, the potential of the positive electrode is assumed to be fixed whilst cycling within a defined window. However, as established in the present study for asymmetric cells made up of an AC negative electrode and an ECP positive electrode, the potential of both electrodes swings during cycling. This view is supported by the asymmetric ECP-AC capacitor introduced by Laforgue et al. [31] who reported that the potential swing of the ECP positive electrode can be as much as 38% of that of the negative electrode. The observed behaviour arises from the pseudo-capacitive nature of the ECP and, as such, the model proposed by Zheng cannot ade-

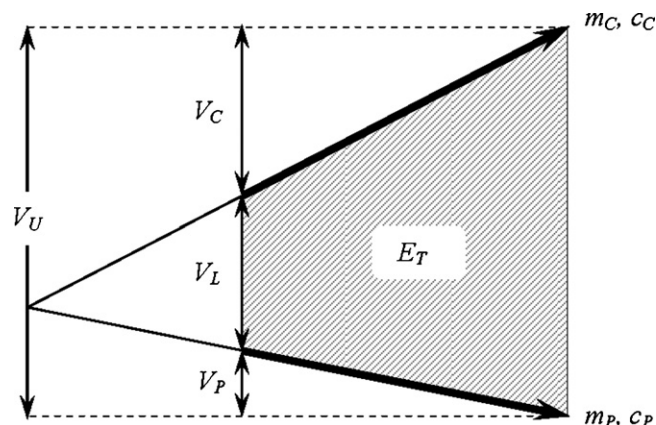


**Fig. 1.** Schematic of potential changes, and origin of parameters used in derived equations, for a hybrid EDLC with a non-Faradaic porous AC electrode and a Faradic ECP electrode. Where,  $E_T$  is the total energy of the cell dependant on the upper limit of the charging voltage ( $V_U$ ) and the lower limit of the discharge voltage ( $V_L$ ). The variables  $V_C$  and  $V_P$  are the swing potentials of the negative and positive electrodes,  $c_C$  is the specific capacitance of the negative electrode and  $c_P$  is the specific capacitance of the positive electrode and  $m_C$  and  $m_P$  are the mass of the active materials in the negative and positive electrodes, respectively.

quately describe such a system. Although more complex models exist [24,28], hybrid supercapacitors with pseudo-capacitive electrodes can also be readily described through the formulation of equations based on capacitance.

In this paper, we derive a series of mathematical formulae as a simplified representation to describe the capacitance observed in redox polymeric materials. The derived equations also predict the maximum specific capacitance for the combination of two dissimilar electrodes assembled in series and the electrode mass ratios required for optimum performance. Through an understanding of the relationship between cell capacitance and electrode (active materials) mass ratios, maximum specific energy and electrode potential swing can also be derived to understand further the function of asymmetric ECP supercapacitors.

## 2. Results

### 2.1. Maximum gravimetric capacitance

A representation of the changes (upon charging) of cell voltage and individual electrode potentials for an asymmetric supercapacitor is depicted in Fig. 1. In this cell, the negative electrode consists of porous activated carbon and the active material of the positive electrode is an ECP that is capable of undergoing positive ion doping. If the cell is cycled within a stable potential window for the reversible doping and de-doping of ECP in the positive electrode, then the rapid redox process essentially parallels the physical adsorption/desorption of ions occurring at the opposite carbon electrode. Consequently the ECP electrode behaves in a *pseudo-capacitive* manner.

As a first approximation, this class of cell assembly can simplistically be treated as two (dissimilar) capacitors in series. Assuming two capacitors in series, where the capacitance of the negative (carbon) electrode is  $C_C$  (F) and that of the positive (polymer) electrode is  $C_P$  (F), the total capacitance,  $C_T$  (F), is given by

$$\frac{1}{C_T} = \frac{1}{C_C} + \frac{1}{C_P} \quad (3)$$

Note that this approach can equally be applied to an 'asymmetric' activated carbon EDLC where the specific capacitances of the positive and negative electrodes are dissimilar due to the qual-

ity/quantity of carbon at each electrode, or in an electrolyte system where the dissimilar size of the positive and negative ions results in disproportionate capacitances at each electrode [32].

Substituting  $m_C$  and  $m_P$  as the mass of the active materials in the negative and positive electrodes, respectively, into Eq. (3), and using the electrode specific capacitances ( $F g^{-1}$ ), then solving for total cell capacitance,  $C_T$  (F), with respect to the active mass of the polymer,  $m_P$ , yields:

$$\frac{C_T}{m_P} = \frac{c_P c_C}{c_C + (m_P/m_C)c_P} \quad (4)$$

where  $c_C$  is the specific capacitance of the negative electrode and  $c_P$  is the specific capacitance of the positive electrode. Performing this substitution and subsequent rearrangement allows us to obtain expressions that include the mass ratio,  $\gamma$ , where  $\gamma = m_P/m_C$  (*vide infra*).

The expression from Eq. (4) relates the total cell capacitance ( $C_T$ ) per mass of positive electrode ( $m_P$ ) in terms of the specific capacitance of the active material of the positive electrode ( $c_P$ ) and the negative electrode ( $c_C$ ) and hence the mass ratio of these electrodes,  $\gamma$ . This is an important derivation that can be used to project the expected total specific capacitance relative to a given mass ratio.

Similarly, the expression can be solved for capacitance per mass of negative electrode, yielding:

$$\frac{C_T}{m_C} = \frac{c_P c_C}{c_P + (c_C/\gamma)} \quad (5)$$

Inclusion of the total active material mass where  $m_T = m_P + m_C$ , which can also be expressed by expansion and reorganisation as  $m_P = m_T/(1 + (1/\gamma))$  and subsequent substitution into Eq. (4) gives the total cell gravimetric capacitance,  $c_T$ , where  $c_T = C_T/m_T$ , expressed as

$$c_T = \frac{c_P c_C / (c_C + (\gamma c_P))}{1 + (1/\gamma)} \quad (6)$$

## 2.2. Optimisation of gravimetric mass ratio for electrode utilisation

Differentiating Eq. (6) with respect to mass ratio,  $\gamma$ , and equating to zero yields the electrode mass ratio that achieves the maximum value of  $c_T$ :

$$\gamma_{\max} = \sqrt{\frac{c_C}{c_P}} \quad (7)$$

The above relationship is useful for obtaining an estimate of the optimum gravimetric electrode mass ratios over a range of possible ECP electrode specific capacitances ( $c_P$ ) using a fixed specific capacitance for the negative AC electrode ( $c_C$ ). The maximum mass ratio, as a function of  $c_P$ , for the examples where  $c_C = 130 F g^{-1}$  (for AC in a non-aqueous electrolyte) or  $200 F g^{-1}$  (aqueous electrolyte) is depicted in Fig. 2(a). It is quite apparent that this relationship is non-linear, thus the choice of the optimum mass ratio required to maximise the total specific cell capacitance is more complex than simply balancing electrode capacitances. Unsurprisingly, the plot indicates that the greater the specific capacitance of the positive active material, the lower the mass ratio and hence the required mass of positive active material is greatly reduced. Similarly, for a carbon electrode with increased capacitance, for example  $200 F g^{-1}$ , the mass ratio increases and correspondingly, the required mass of positive active material also increases.

In a similar manner, this calculation can be performed for a fixed value of  $c_P$ , say 250 and  $500 F g^{-1}$ , as depicted in Fig. 2(b). As discussed above, the increase is non-linear with an inverse relationship and the gravimetric requirement for positive active material is significantly less, especially when the ECP has a disproportionately large capacitance, for example polyaniline. Intuitively, due consideration must be taken when using this relationship as the capacitance of AC is generally limited [5].

Substituting the maximum gravimetric ratio from Eq. (7) into Eq. (6), the maximum capacitance ( $c_T$ ) can be obtained for the positive electrode over a range of  $c_P$ . This relationship for an example where  $c_C = 130$  and  $200 F g^{-1}$  is shown in Fig. 3. In this asymmetric configuration, the relationship approaches a limit as  $c_P$  becomes increasingly larger than  $c_C$  and thus further increases become less important.

In a similar manner, examining the rate of change of maximum  $c_T$  with respect to  $c_P$  will give maximum utilisation of the positive electrode. As a further example, the maximum specific capacitance ( $c_T$ ) obtainable for the positive electrode over a range of  $c_C$  when  $c_P = 250$  and  $500 F g^{-1}$  is shown in Fig. 4. Variation in  $c_C$  has a less evident (yet still significant) effect on maximum  $c_T$  at high values of  $c_C$ ; the implication is that to achieve maximum cell specific capacitance, it is of critical importance to maximise the carbon electrode specific capacitance.

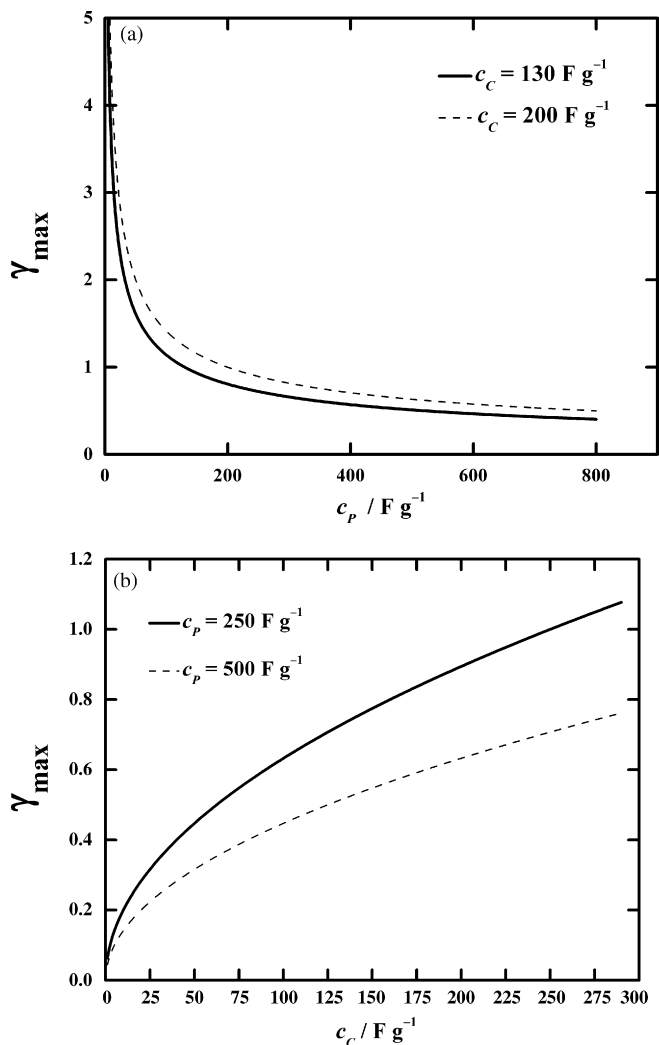


Fig. 2. (a) Maximum electrode mass ratio,  $\gamma$ , as function of capacitance of positive electrode,  $c_P$ , for two negative electrode capacitances,  $c_C = 130$  and  $200 F g^{-1}$ . (b) Maximum electrode mass ratio,  $\gamma$ , as function of capacitance of negative electrode,  $c_C$ , for two positive electrode capacitances,  $c_P = 250$  and  $500 F g^{-1}$ .

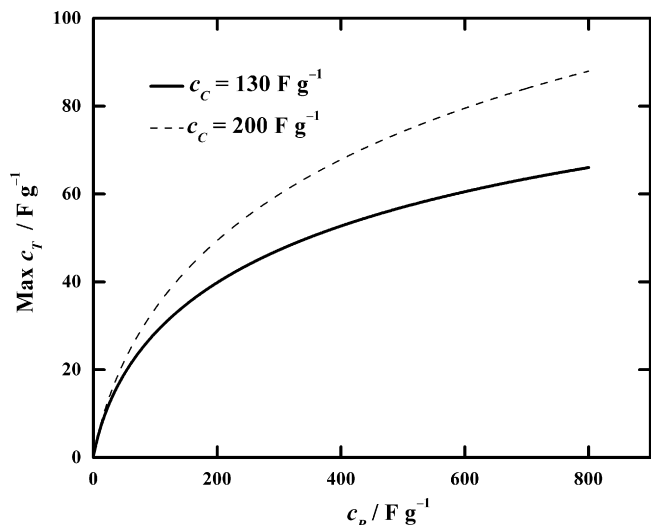


Fig. 3. Maximum total capacitance,  $c_T$ , as function of capacitance of positive electrode,  $c_p$ , for two negative electrode capacitances,  $c_c = 130$  and  $200 \text{ F g}^{-1}$ .

### 2.3. Specific energy

Under galvanostatic charge and discharge of a capacitor, the energy of the cell can be calculated according to Eq. (8) [33,34]:

$$E = i \int V dt \quad (8)$$

where  $i$  is the current density, and  $V$  is the cell voltage during discharge. The latter can be represented by the shaded region of Fig. 1 ( $E_T$ ) and will be dependant on both the upper limit of the charging voltage ( $V_U$ ) and the lower limit of the discharge voltage ( $V_L$ ).

Considering the maximum total capacitance  $c_T$  obtained in Eq. (6) and if the upper voltage limit corresponds to the maximum voltage  $V_M$ , (i.e.,  $V_U = V_M$ ), then the maximum stored energy based on active material weight ( $\text{Wh kg}^{-1}$ ) of a symmetric or asymmetric supercapacitor, is given by

$$E_{\max} = \frac{1/2 c_T V_M^2}{3.6} \quad (9)$$

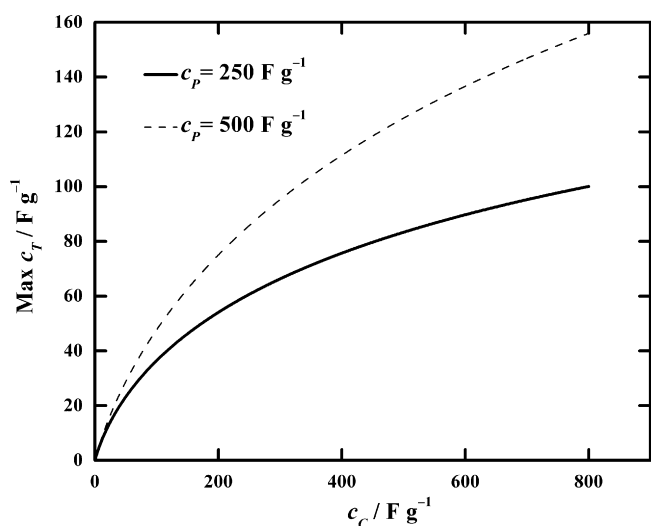


Fig. 4. Maximum total capacitance,  $c_T$ , as function of capacitance of negative electrode,  $c_c$ , for two positive electrode capacitances,  $c_p = 250$  and  $500 \text{ F g}^{-1}$ .

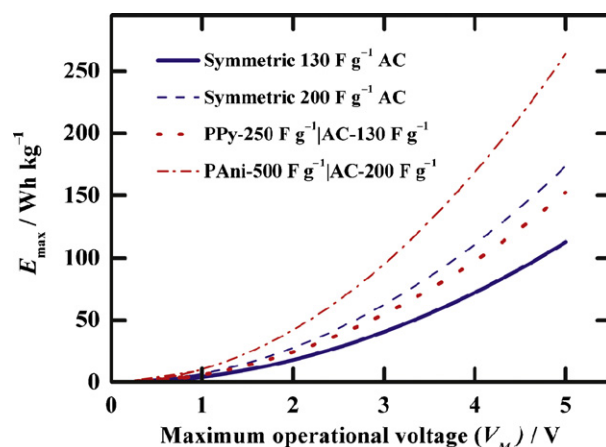


Fig. 5. Maximum specific energy,  $E_{\max}$ , as function of maximum operational voltage,  $V_M$ , for a series of indicated symmetric and asymmetric EDLC systems.

The relationship between  $V_M$  and  $E_{\max}$  for two representative symmetric EDLCs (each based on 130 or  $200 \text{ F g}^{-1}$  carbon electrodes) and two asymmetric ECP-AC supercapacitors, where one of the carbon electrodes is replaced with an ECP electrode (PPy or PAni) is depicted in Fig. 5. This highlights the impact of the asymmetric configuration on calculated  $E_{\max}$ , at representative  $V_M$  (obtained from typical literature values) for the different systems. For a given carbon electrode, the asymmetric ECP-AC combination enables greater energy storage capacities to be achieved and, as expected, in all cases  $E_{\max}$  increases rapidly with increasing  $V_M$ . Clearly even symmetric EDLCs are substantially enhanced by a modest increase in  $V_M$ , however the most significant improvements in  $E_{\max}$  are obtained when both an increased capacitance (from an asymmetric configuration) and increased cell voltage are utilised. An asymmetric PPy-AC supercapacitor, operating a 3.5 V, could store  $\sim 74 \text{ Wh kg}^{-1}$  (based on the active material weight only) which is  $\sim 35\%$  higher than the equivalent symmetric carbon system as shown in Fig. 5.

The advantage of a high operating  $V_M$ , indicated by the data presented in Fig. 5, would allow increased utilisation in such applications as portable devices and hybrid electric vehicles. It is not a trivial matter, however, to identify a supercapacitor electrolyte-electrode system, capable of operating at high voltages ( $>3 \text{ V}$ ) whilst still maintaining performance (over a wide temperature range) and long-term stability. There is currently much interest in the application of room temperature ionic liquids (RTILs) as alternative electrolytes in supercapacitors, with many exhibiting a wide potential window; some in excess of 5 V [35].

### 2.4. Electrode swing potential in asymmetric hybrid cells

The charge on the negative and positive electrodes, respectfully, is given by

$$Q_C = m_C c_C V_C \quad (10)$$

$$Q_P = m_P c_P V_P \quad (11)$$

where  $V_C$  and  $V_P$  are the swing potentials of the negative and positive electrodes, respectively, and  $V_S$  can be defined as the swing voltage of the cell during charging, namely:  $V_S = V_C + V_P$  (see Fig. 1). Considering the charge-balance relationship,  $Q_P = Q_C$ , the percentage of  $V_S$  contributed by the negative electrode is given by

$$V_C = \frac{C_P}{C_P + C_C} 100 \quad (12)$$

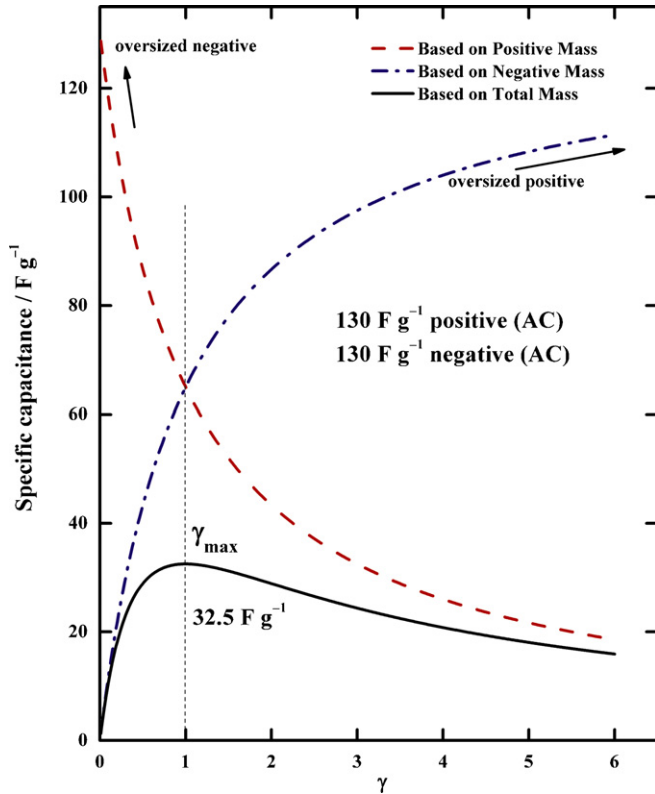


**Fig. 6.** For a symmetric EDLC where  $c_C = c_P = 130 \text{ F g}^{-1}$  maximum total capacitance,  $c_T$ , as function of electrode mass ratio,  $\gamma$ , with respect to positive,  $m_P$ , negative,  $m_C$ , and total,  $m_T$ , electrode masses as indicated in the figure. The dotted vertical line indicates optimum value of  $\gamma$ ,  $\gamma_{\max}$ .

Substituting active material masses, specific capacitances and simplifying yields:

$$V_C = \frac{c_P}{c_P + (c_C/\gamma)} 100 \quad (13)$$

Similarly, the percentage of  $V_S$  contributed by the positive electrode is given by

$$V_P = \frac{c_C}{(c_P \gamma) + c_C} 100 \quad (14)$$

Equating (13) with (14) gives the electrode mass ratio for when both electrodes swing symmetrically, *i.e.*,  $V_C = V_P = 50\% V_S$ :

$$\frac{c_P}{c_P + (c_C/\gamma)} = \frac{c_C}{(c_P \gamma) + c_C} \quad (15)$$

Rearranging Eq. (15) with respect to mass ratio yields:

$$c_P c_C + (c_P^2 \cdot \gamma) = c_C c_P + (c_C^2/\gamma) \quad (16)$$

and further simplification gives

$$\gamma = \frac{c_C}{c_P} \quad (17)$$

A plot (not shown here) of Eq. (17) for equal capacitance electrodes ( $c_C = c_P$ ) gives the expected results for symmetric EDLC electrodes where the swing voltage is equally distributed across each electrode and, therefore, is consistent for describing these systems.

### 3. Discussion

#### 3.1. Symmetric activated carbon EDLC cell

Symmetric cells can be formed with two identical porous carbon electrode in either: non-aqueous electrolyte (*e.g.*, 1 M tetraethylammonium tetrafluoroborate ( $\text{NET}_4\text{BF}_4$ ) in propylene carbonate (PC)); or in aqueous electrolyte (*e.g.*, 1 M  $\text{H}_2\text{SO}_4$ ). As an example, using a capacitance value of  $130 \text{ F g}^{-1}$  for a carbon electrode in a non-aqueous electrode, the theoretical capacitance of a symmetric AC system, as a function of mass ratio ( $\gamma$ ), were calculated using Eqs. (4)–(6) and a representative plot for the non-aqueous system is displayed in Fig. 6. The results confirm that, irrespective of the electrolyte system used, and independent of voltage, the derived equations replicate the predictable properties that would be expected for these two recognised AC systems. First, the optimum mass ratio ( $\gamma$ ) is obtained at 1.0. Second, the optimum gravimetric capacitance,  $c_T$ , is one-quarter the capacitance of a single electrode, *i.e.*,  $32.5 \text{ F g}^{-1}$ , for the non-aqueous system and  $50 \text{ F g}^{-1}$  (not shown) for the aqueous system (assuming  $200 \text{ F g}^{-1}$ ). Hence, the case when  $C_1 = C_2$ , gives the expected relationship,  $c_T = \frac{1}{2} C_1$  irrespective of electrode mass.

The plot of specific energy,  $E$  ( $\text{Wh kg}^{-1}$ ), as a function of  $\gamma$ , for the two symmetric carbon EDLC systems is shown in Fig. 7(a). Using nominal values of  $V_M$  (for non-aqueous = 3.0 V, and for aqueous = 1.5 V), Fig. 7(a) indicates an optimum electrode mass ratio of

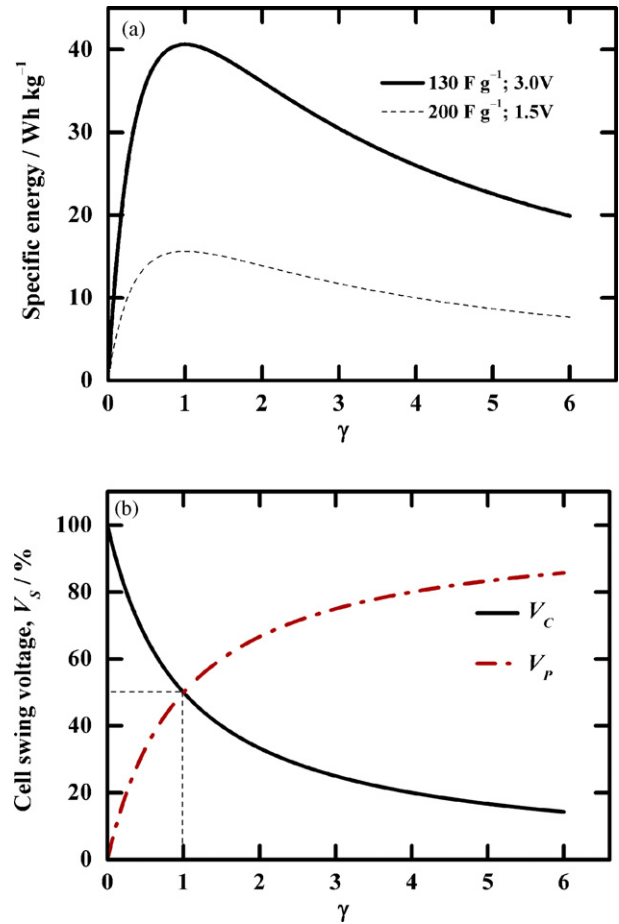


**Fig. 7.** (a) Specific energy ( $\text{Wh kg}^{-1}$ ) as function of electrode mass ratio,  $\gamma$ , for symmetric EDLCs for (i)  $c_C = c_P = 130 \text{ F g}^{-1}$ ,  $V_M = 3.0 \text{ V}$ ; (ii)  $c_C = c_P = 200 \text{ F g}^{-1}$ ,  $V_M = 1.5 \text{ V}$ , as indicated in the figure. (b) Proportion of cell swing voltage (%) on negative,  $V_C$ , and positive,  $V_P$ , electrodes as function of electrode mass ratio,  $\gamma$ , as indicated in the figure.

1.0 and a corresponding maximum specific energy of  $40.6 \text{ Wh kg}^{-1}$  for a non-aqueous cell and  $15.6 \text{ Wh kg}^{-1}$  for an aqueous cell. In addition, the swing potential for the respective positive and negative electrodes, as a function of  $\gamma$ , also correlates with these predictions giving a swing of 50% on each electrode (Fig. 7(b)).

### 3.2. Asymmetric ECP-AC cells

#### 3.2.1. Aqueous carbon-polyaniline cell

For an asymmetric supercapacitor cell constructed from a porous activated carbon negative electrode with a specific capacitance of  $200 \text{ F g}^{-1}$ , a PANi positive electrode with a specific capacitance of  $500 \text{ F g}^{-1}$  in  $1 \text{ M H}_2\text{SO}_4$ , the theoretical capacitance from Eqs. (4) to (6) for these cell parameters, as a function of  $\gamma$ , is presented in Fig. 8(a). Whilst the curves from Eqs. (4) and (5) describe the capacitance limits for gravimetric oversized positive and negative electrodes, respectively, the resultant function from Eq. (6), i.e., the capacitance plotted with respect to the total electrode mass  $c_T$ , is most informative. The curve depicts the optimum gravimetric mass ratio to obtain the maximum total specific capacitance per total mass ( $c_T, \text{ F g}^{-1}$ ). Further detailed examination of Fig. 8(a) indicates that the predicted maximum specific capacitance is  $75 \text{ F g}^{-1}$  and occurs at  $\gamma = 0.65$ .

Confirmation of the validity of this approach can be found by observing the limits of Eqs. (4) and (5) for the respective positive and negative electrodes at the derived mass ratios. At low  $\gamma$ , where the negative electrode is oversized, the capacitance per positive active material mass ( $c_p$ ) approaches that of the positive electrode ( $500 \text{ F g}^{-1}$ ). Conversely, at high  $\gamma$  where the positive electrode is sufficiently oversized, the capacitance per negative active material mass ( $c_c$ ) approaches that of the negative electrode ( $200 \text{ F g}^{-1}$ ).

#### 3.2.2. Non-aqueous carbon-polypyrrole cell

A second illustrative asymmetric hybrid EDLC cell can be formed from a porous activated carbon negative electrode with a specific capacitance of  $130 \text{ F g}^{-1}$ , a PPy positive electrode with a specific capacitance of  $250 \text{ F g}^{-1}$  in  $1 \text{ M NEt}_4\text{BF}_4$  in PC. Similarly to that described above, the functions from Eqs. (4) to (6) for these cell parameters with respect to  $\gamma$  gives the data displayed in Fig. 8(b). From this set of data, the predicted maximum gravimetric capacitance is  $\sim 43.5 \text{ F g}^{-1}$ , where  $\gamma = 0.72$ . This indicates that a 70% improvement in total specific capacitance for a cell is gained when using PANi with  $c_p = 500 \text{ F g}^{-1}$  (see Fig. 8(a)) as opposed to PPy where  $c_p$  of the positive electrode =  $250 \text{ F g}^{-1}$ . Superficially this would appear to be a significant enhancement to the resultant device; however, there are several other factors that should also be considered. These include the cell operating voltage (non-aqueous electrolytes allow  $>2.5 \text{ V}$  operating voltages and hence a higher stored energy) and the comparable  $\gamma$ . An optimum mass ratio will impact the end device's energy density as well as associated power and cycle-life performance due to the different proportion of ECP in the matched cell.

It is also apparent from Fig. 8(a) that achieving an optimum mass ratio for a PANi-AC cell is more critical due to the capacitance imbalance of  $c_p \gg c_c$ . (cf. PPy and AC in non-aqueous electrolyte, Fig. 8(b)). Conversely, if a poor quality activated carbon was chosen for the negative electrode with  $c_c = 130 \text{ F g}^{-1}$ , the improvement in total capacitance for PANi as a positive active material is more modest as  $c_T$  changes from  $75$  to  $57 \text{ F g}^{-1}$  (only a 30% improvement cf. 70% above) and a corresponding change in  $\gamma$  from  $0.65$  to  $0.49$ . Thus to achieve optimum performance from PANi, with its much higher  $c_p$ , requires a porous activated carbon  $\gg 200 \text{ F g}^{-1}$  which is toward the upper limit of the experimentally attainable capacitance for this material [5]. An alternative consequence may mean that, although

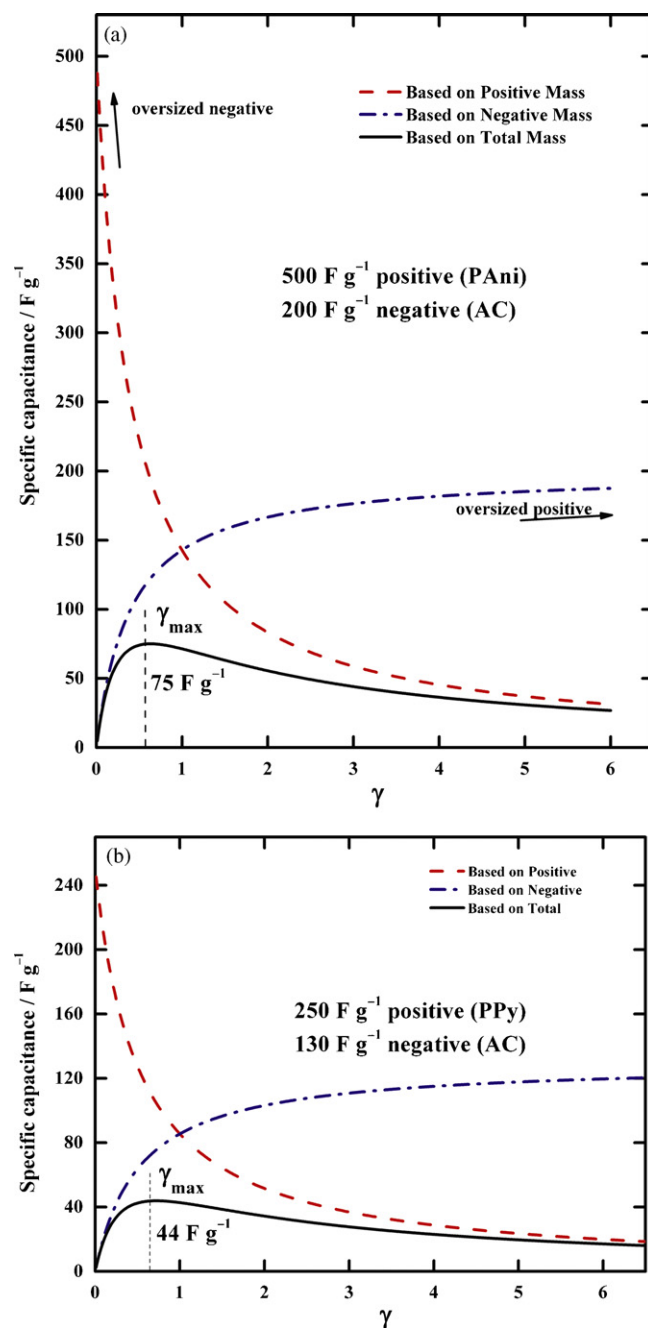
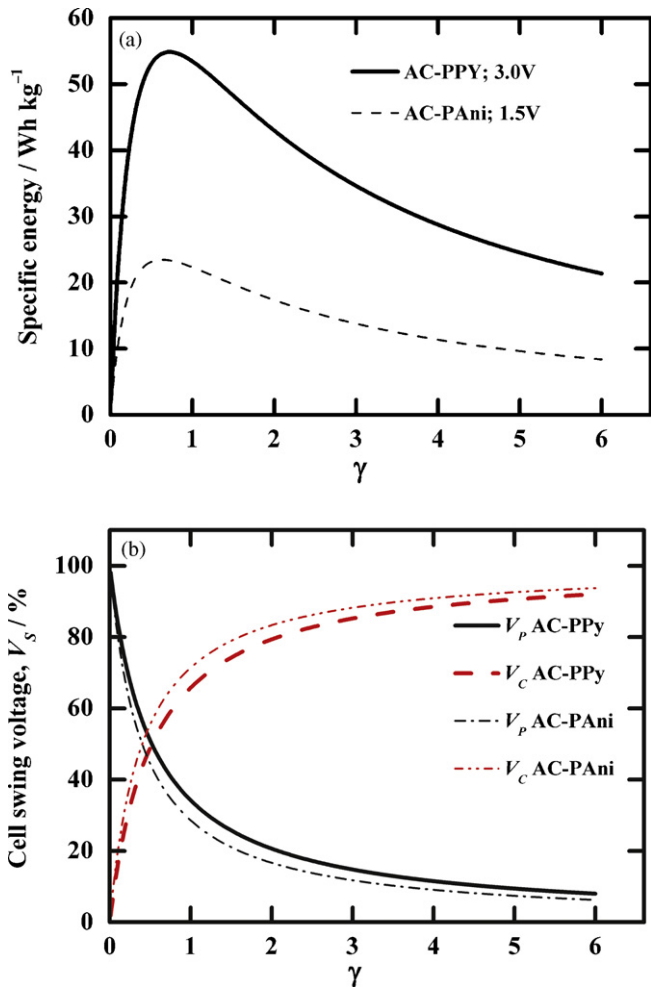


Fig. 8. (a) Asymmetric PANi-AC EDLC where  $c_c = 200 \text{ F g}^{-1}$ ,  $c_p = 500 \text{ F g}^{-1}$ . (b) Asymmetric PPy-AC EDLC where  $c_c = 130 \text{ F g}^{-1}$ ,  $c_p = 250 \text{ F g}^{-1}$ . Showing maximum total capacitance,  $c_T$ , as function of electrode mass ratio,  $\gamma$ , with respect to positive,  $m_p$ , negative,  $m_c$ , and total,  $m_T$ , electrode masses as indicated in the figure. Dotted vertical line indicates optimum value of  $\gamma$ ,  $\gamma_{\text{max}}$ .

a lower overall cell  $c_T$  is achieved with PPy, a more optimised cell can be formed due to the closer matching of the two capacitive materials.

### 3.3. Specific energy

Relative improvements in the stored specific energy (on an active materials basis) for the PANi-AC and PPy-AC asymmetric cells are depicted as the dashed and solid lines in Fig. 9(a), respectively. A specific energy of  $54.8 \text{ Wh kg}^{-1}$  is predicted for the PPy-AC asymmetric cell, which is a 35% improvement over the comparable



**Fig. 9.** (a) Specific energy ( $\text{Wh kg}^{-1}$ ) as function of electrode mass ratio,  $\gamma$ , for asymmetric EDLCs where (i)  $c_c = 130 \text{ F g}^{-1}$ ,  $c_p = 250 \text{ F g}^{-1}$ , and  $V_M = 3.0 \text{ V}$ ; (ii)  $c_c = 200 \text{ F g}^{-1}$ ,  $c_p = 500 \text{ F g}^{-1}$ , and  $V_M = 1.5 \text{ V}$ . (b) Proportion of cell swing voltage (%) on negative,  $V_c$ , and positive,  $V_p$ , electrodes as function of electrode mass ratio,  $\gamma$ . Solid lines are for system (i) and dotted lines are for system (ii) and are indicated in the figure.

non-aqueous (3 V) symmetric EDLC, and would predictably have an improvement of >130% over the aqueous AC-PAni (1.5 V) cell. At the optimum mass ratio, the respective electrode swing potentials, plotted in Fig. 9(b), are also predicted to have deviated from the symmetric cell with  $V_c = 58\%$  and  $V_p = 42\%$  (of the total cell swing voltage respectively) which is a shift in the  $\pm$  swing ratio due to the reduced capacitance ECP *cf.* PAni, yet still shows a significant improvement over symmetric EDLCs.

A specific energy of  $23.4 \text{ Wh kg}^{-1}$  is predicted for the PAni-AC system (dashed line in Fig. 9(a)), which is a 50% improvement over the comparable aqueous (1.5 V) symmetric EDLC. Additionally, the electrode swing potentials (Fig. 9(b)), are also predicted to have deviated from the symmetric cell with  $V_c = 62\%$  and  $V_p = 38\%$  indicating that the increased capacitance from the positive electrode is directing the improvement in specific energy.

Wang et al. [36] have constructed an asymmetric supercapacitor based on the PAni-AC system, where  $c_c = 160 \text{ F g}^{-1}$ ,  $c_p = 420 \text{ F g}^{-1}$  and  $V_M = 1.4 \text{ V}$ . Using these reported parameters, a  $C_T$  of  $61.1 \text{ F g}^{-1}$  at  $\gamma = 0.62$ , is predicted which corresponds to a maximum specific energy of  $16.6 \text{ Wh kg}^{-1}$ . Our predicted value correlates well to the experimentally measured value of  $15.5 \text{ Wh kg}^{-1}$  and also suggests that the experimental mass ratio was slightly less than the predicted optimised ratio; indicating that the cell had a slightly oversized AC electrode.

#### 3.4. Non-aqueous carbon-poly-4-fluorophenylthiophene (P-4-FT) asymmetric cell

An illustrative experimental asymmetric supercapacitor is that introduced by Laforgue et al. [31] where they report on a 2600 F prismatic prototype (SC-03) with a specific energy of  $7.49 \text{ Wh kg}^{-1}$  (for the sealed prototype) at a maximum operational voltage of 3.0V. The cell consisted of a porous activated carbon negative electrode with a specific capacitance of  $130 \text{ F g}^{-1}$  and a poly-4-fluorophenylthiophene positive electrode with a specific capacitance of  $245 \text{ F g}^{-1}$  in 1 M  $\text{NET}_4\text{BF}_4$  in PC. From the data supplied,  $m_p = 37.6 \text{ g}$ ,  $C_T = 2600 \text{ F}$  and the gravimetric ratio  $\gamma = 1.58$ ; hence the remaining experimentally derived parameters can be

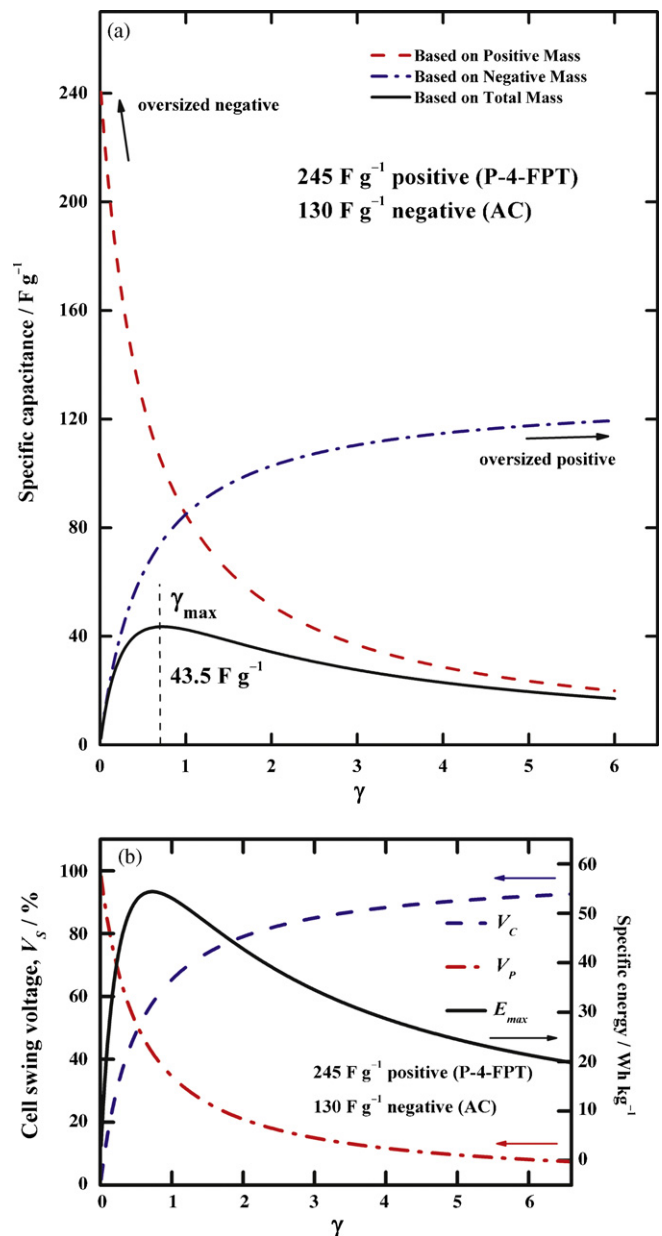


**Fig. 10.** For a asymmetric EDLC where  $c_c = 130 \text{ F g}^{-1}$ ,  $c_p = 245 \text{ F g}^{-1}$ , and  $V_M = 3.0 \text{ V}$  showing (a) maximum total capacitance,  $C_T$ , as function of electrode mass ratio,  $\gamma$ , with respect to positive,  $m_p$ , negative,  $m_c$ , and total,  $m_T$ , electrode masses as indicated in the figure. The dotted vertical line indicates  $\gamma_{\text{max}}$ . (b) (i) Specific energy ( $\text{Wh kg}^{-1}$ ) (right axis); (ii) proportion of cell swing voltage (%) on negative,  $V_c$ , and positive,  $V_p$ , electrodes (left axis) as function of electrode mass ratio,  $\gamma$ .

calculated as:  $m_C = 23.8 \text{ g}$ ,  $c_T = 42.3 \text{ F g}^{-1}$  and  $E_{\max} = 52.9 \text{ Wh kg}^{-1}$  (active materials only).

Using these published electrode and cell parameters in the derived functions, Eqs. (4)–(6), yield the data plotted in Fig. 10(a) and (b). The optimum electrode mass ratio for this system is calculated to be 0.73 and corresponds to  $c_T = 43.5 \text{ F g}^{-1}$  (Fig. 10(a)). Such a cell would be expected to have an  $E_{\max}$  of  $54.4 \text{ Wh kg}^{-1}$  (Fig. 10(b)) and therefore, it would appear that the cell reported by Laforgue et al. was not optimised for maximum specific energy. Their high mass ratio ( $\gamma = 1.58$ ) indicates that the cell employs a gravimetrically oversized positive electrode; possibly to extend the cell cycle-life by reducing the swing potential across the positive electrode. This is supported by the high number of galvanostatic cycles reported (>7500 cycles) and also by investigating the relative swing of the positive and negative electrodes (Fig. 10(b)). Our derived expressions suggests that for optimum specific energy,  $V_C = 58\%$  and  $V_P = 42\%$ , which for the voltage range utilised by Laforgue et al. (1.2–3.0 V) gives  $V_S = 1.8 \text{ V}$  and corresponds to  $V_C = 1.044 \text{ V}$  and  $V_P = 0.756 \text{ V}$ . Laforgue et al. report electrode swings of a swing of  $V_C = 1.3 \text{ V}$  and  $V_P = 0.5 \text{ V}$ , these swings correspond to 72.2% and 27.8%, respectively, of  $V_S$  which is a more modest utilisation of the positive electrode; a technique commonly employed to extend cell lifetime [37,38]. In addition, from our derivations, this swing voltage split suggests that  $\gamma$  for the hybrid cell reported by Laforgue et al. was greater than the optimised value, but less than that reported (1.58), indicating that the capacitance of ECP is not fully utilised (i.e., the effective  $c_P < 245 \text{ F g}^{-1}$ ) under the repeated galvanostatic charging conditions reported.

#### 4. Conclusions

Starting from the equations routinely used to describe conventional symmetric EDLCs, mathematical functions have been derived that can effectively describe the operational and performance characteristics of asymmetric ECP–AC supercapacitors. The derived mathematical formulae are demonstrated to predict cell parameters for a number of theoretical hybrid ECP–AC systems and correlated with experimentally obtained parameters of similar ECP–AC cells. Our mathematical approach incorporated the potential swing across the positive (or redox) electrode and indeed has confirmed that the potential swing across such electrodes, in an asymmetric cell configuration, is significant and needs to be taken into account.

The predictive capability of the derived expressions allows the incorporation of experimentally or empirically obtained starting parameters (e.g., specific material capacitances) and to use these as a means for guiding the optimisation of electrode mass ratio, positive and negative electrode swing voltages, which, in turn, permits the maximum specific energy of a cell to be reliably determined. The broad utility of these series of derived functions allows the prediction of essential cell parameters irrespective of the electrolyte ion concentration, solvent or species and independent of voltage.

In our experience there are two approaches to device optimisation, namely: (i) attaining maximum specific energy; and (ii) stabilisation for extended cycle-life. Operating a cell at  $\gamma_{\max}$  will deliver the maximum specific energy but involves a trade-off in cycle-life. Under these conditions to attain maximum cell capacitance, often the positive ECP electrode may swing significantly and this leads to limited cycle-life. Oversizing the negative carbon electrode increases the proportion of voltage swing experienced at this electrode and will lead to a less-than-optimum specific energy

of the cell, but this electrode is well suited to long-term cycling. By limiting the swing on the positive ECP electrode cycle-life is extended as the active material associated with this electrode is prone to early failure due to volume expansion and/or degradation during the redox process. The formulations outlined here seek to assist those interested in cell optimisation on how best to obtain these goals, and act as a guideline to determine electrode and cell performance.

#### Acknowledgements

This work has been supported by the CSIRO Energy Transformed Flagship initiative. The authors would like to also thank Dr. Noel Duffy and Dr. Tony Hollenkamp for many informative discussions and Dr. David Rand for his assistance in the preparation of this manuscript.

#### References

- [1] B.E. Conway, *Electrochemical Supercapacitors*, Kluwer Academic/Plenum, New York, 1999.
- [2] M. Nakamura, M. Nakanishi, K. Yamamoto, *J. Power Sources* 60 (1996) 225.
- [3] D.Y. Qu, H. Shi, *J. Power Sources* 74 (1998) 99.
- [4] M. Endo, T. Takeda, Y.J. Kim, K. Koshiba, K. Ishii, *Carbon Sci.* 1 (2001) 117.
- [5] A. Lewandowski, M. Galinski, *J. Power Sources* 173 (2007) 822.
- [6] K. Jurewicz, C. Vix-Guterl, E. Frackowiak, S. Saadallah, A. Reda, J. Parmentier, J. Patarin, F. Beguin, *J. Phys. Chem. Solids* 65 (2004) 287.
- [7] J. Chmiola, G. Yushin, Y. Gogotsi, C. Portet, P. Simon, P.L. Taberna, *Science* 313 (2006) 1760.
- [8] B.E. Conway, *J. Electrochem. Soc.* 138 (1991) 1539.
- [9] G.G. Amatucci, F. Badway, A. Du Pasquier, T. Zheng, *J. Electrochem. Soc.* 148 (2001) A930.
- [10] A.I. Belyakov, A.M. Brintsev, *International Seminar on Double Layer Capacitors and Similar Energy Storage Devices*, Florida Educational Seminars, 1997.
- [11] G. Thomas, Motorola Inc. (Moti), WO9521466-A; US5429893-A; WO9521466-A1, 1994.
- [12] A. Burke, *J. Power Sources* 91 (2000) 37.
- [13] B.E. Conway, V. Birss, J. Wojtowicz, *J. Power Sources* 66 (1997) 1.
- [14] B.E. Conway, W.G. Pell, *J. Solid State Electrochem.* 7 (2003) 637.
- [15] G.A. Snook, G.Z. Chen, D.J. Fray, M. Hughes, M. Shaffer, *J. Electroanal. Chem.* 568 (2004) 135.
- [16] M. Mastragostino, F. Soavi, C. Arbizzani, *Advances in Li-ion Batteries*, Kluwer Academic/Plenum, New York, 2002, p. 481.
- [17] P. Novak, K. Muller, K.S.V. Santhanam, O. Haas, *Chem. Rev.* 97 (1997) 207.
- [18] C. Arbizzani, M. Mastragostino, L. Meneghello, R. Paraventi, *Adv. Mater.* 8 (1996) 331.
- [19] D. Villers, D. Jobin, C. Soucy, D. Cossement, R. Chahine, L. Breaud, D. Belanger, *J. Electrochem. Soc.* 150 (2003) A747.
- [20] K.S. Ryu, K.M. Kim, Y.J. Park, N.G. Park, M.G. Kang, S.H. Chang, *Solid State Ionics* 152 (2002) 861.
- [21] S.A. Hashmi, H.M. Upadhyaya, *Solid State Ionics* 152 (2002) 883.
- [22] Y.M. Volfkovich, T.M. Serdyuk, *Russ. J. Electrochem.* 38 (2002) 935.
- [23] G.A. Snook, G.Z. Chen, *J. Electroanal. Chem.* 612 (2008) 140.
- [24] W.G. Pell, B.E. Conway, *J. Power Sources* 136 (2004) 334.
- [25] T.R. Jow, J.P. Zheng, *J. Electrochem. Soc.* 145 (1998) 49.
- [26] X. Wang, J.P. Zheng, *J. Electrochem. Soc.* 151 (2004) A1683.
- [27] J.P. Zheng, J. Huang, T.R. Jow, *J. Electrochem. Soc.* 144 (1997) 2026.
- [28] J.P. Zheng, *J. Electrochem. Soc.* 150 (2003) A484.
- [29] J.P. Zheng, *J. Electrochem. Soc.* 152 (2005) A1864.
- [30] S.A. Kazaryan, S.N. Razumov, S.V. Litvinenko, G.G. Kharisov, V.I. Kogan, *J. Electrochem. Soc.* 153 (2006) A1655.
- [31] A. Laforgue, P. Simon, J.F. Fauvarque, J.F. Sarrau, P. Lailier, *J. Electrochem. Soc.* 148 (2001) A1130.
- [32] Y.H. Wen, J. Cheng, G.P. Cao, Y.H. Yang, *J. Appl. Electrochem.* 37 (2007) 543.
- [33] A. Laforgue, P. Simon, J.F. Fauvarque, M. Mastragostino, F. Soavi, J.F. Sarrau, P. Lailier, M. Conte, E. Rossi, S. Saguatti, *J. Electrochem. Soc.* 150 (2003) A645.
- [34] H. Talbi, P.E. Just, L.H. Dao, *J. Appl. Electrochem.* 33 (2003) 465.
- [35] M. Galinski, A. Lewandowski, I. Stepniak, *Electrochim. Acta* 51 (2006) 5567.
- [36] X.F. Wang, D.B. Ruan, D.Z. Wang, J. Liang, *Acta Phys. Chim. Sinica* 21 (2005) 261.
- [37] L.T. Lam, R. Louey, N.P. Haigh, O.V. Lim, D.G. Vella, C.G. Phyland, L.H. Vu, J. Furukawa, T. Takada, D. Monma, T. Kano, *J. Power Sources* 174 (2007) 16.
- [38] K. Kato, A. Negishi, K. Nozaki, I. Tsuda, K. Takano, *J. Power Sources* 117 (2003) 118.